

# Structure/Calcium Affinity Relationships of Site III of Calmodulin: Testing the Acid Pair Hypothesis Using Calmodulin Mutants<sup>†</sup>

Xiaochun Wu and Ronald E. Reid\*

*Division of Pharmaceutical Chemistry, Faculty of Pharmaceutical Sciences, University of British Columbia, Vancouver, British Columbia V6T 1Z3, Canada*

*Received February 6, 1997; Revised Manuscript Received April 22, 1997<sup>⊗</sup>*

**ABSTRACT:** Calmodulin mutants in which the calcium binding affinity of site IV was greatly reduced by a D133E mutation were prepared using site-specific, cassette-mediated mutagenesis as a multisite calcium binding protein model to examine structure/calcium affinity relationships in site III of calmodulin. Tryptophan was introduced in position 92 of the calmodulin mutants as a fluorescent label to monitor the calcium-induced structural changes in the C-terminal domain of calmodulin. The five calmodulin mutants, 3xCaM, 3zCaM, 4xCaM, 4zCaM, and 4xzCaM, were designed so that there were three or four acidic amino acid residues in chelating positions of site III with acid pairs on either the X and/or Z coordinating axes. The calcium dissociation constant of site III,  $K_{III}$ , of the five calmodulin mutants changes in a descending order from 3xCaM (237  $\mu$ M), 3zCaM (140  $\mu$ M), 4xCaM (5.8  $\mu$ M), 4zCaM (3  $\mu$ M), to 4xzCaM (2  $\mu$ M), and these  $K_{III}$  values are significantly lower than that of F92W/D133E calmodulin (335  $\mu$ M) in which three acidic residues with no acid pairs were present in site III [Wu, X., & Reid, R. E. (1997) *Biochemistry* 36, 3608–3616]. These results indicate that the calcium affinity of site III increases when the number of the acidic chelating residues increases from three to four, when the number of acid pairs increases from zero to one and further to two, and when the location of the acid pair is changed from the X axis to the Z axis. This study provides the first evidence that the acid pair hypothesis which correlates the nature of the chelating residues with the calcium affinity of the hlh motif is applicable to a multisite calcium binding protein model. The Hill coefficients indicate that reversal of the sequence of filling of the calcium binding sites in the C-terminal domain from IV  $\rightarrow$  III to III  $\rightarrow$  IV also changes the site cooperativity from positive to negative. The cooperativity returns to positive when the proteins are titrated in the presence of a calmodulin-binding peptide. Data from the present study also demonstrate that calmodulin mutants with a decreased calcium affinity have a reduced efficiency in phosphodiesterase regulation at low calcium concentrations (50  $\mu$ M). However, high calcium concentrations (15 mM) restore the phosphodiesterase regulatory activity of the calmodulin mutants to a level obtained with F92W calmodulin, indicating that the mutations alter calcium regulation of calmodulin-mediated phosphodiesterase activity without affecting the interaction between calmodulin and the enzyme.

The helix-loop-helix (hlh)<sup>1</sup> calcium-binding motif, also termed “EF hand” by Kretsinger when his group elucidated the structure of carp parvalbumin (1), has been identified in many calcium-binding proteins, including calmodulin (CaM), troponin C, calbindin, and parvalbumin (2, 3). Currently, over 500 examples of the hlh motif have been found in the

protein sequence data base (4). The hlh calcium-binding motif consists of two  $\alpha$ -helices that flank a loop. A 12-residue region comprising the loop and the N-terminal end of the second helix contains the oxygen ligands. The term “loop” will be used in reference to this entire 12-residue region. Six residues located at positions 1, 3, 5, 7, 9, and 12 of the loop interact either directly or indirectly with the calcium ion, and these six positions are denoted as the +X, +Y, +Z, -Y, -X, and -Z positions on the axes of a near-octahedral coordination shell (Figure 1A).

The hlh calcium-binding proteins are a family of highly homologous proteins, the activities of which are regulated by fluctuating levels of calcium within a cell. The calcium dissociation constants of a number of calcium-binding proteins from the CaM superfamily have been reported by different groups, and the values range from 1 nM to 0.1 mM, although the sequences of the hlh calcium binding sites are highly homologous (5). Several investigators have tried to predict calcium binding properties of the hlh motif or paired motifs on the basis of their amino acid sequences. Potter et al. found that a Gly residue is usually located between the +Y and +Z chelating residues in loops with a low calcium

<sup>†</sup> This study was funded by Operating Grant MT-11647 from the Medical Research Council of Canada. X.W. was supported by PMAC-HRF/MRC Graduate Research Scholarship of Canada.

\* Corresponding author: Ronald E. Reid, Ph.D., 2146 East Mall, Faculty of Pharmaceutical Sciences, University of British Columbia, Vancouver, BC V6T 1Z3, Canada. Telephone: (604) 822-4706. Fax: (604) 822-3035. E-mail: calm@unixg.ubc.ca.

<sup>⊗</sup> Abstract published in *Advance ACS Abstracts*, June 15, 1997.

<sup>1</sup> Abbreviations: CaM, calmodulin; hlh, helix-loop-helix; APH, acid pair hypothesis; VU-1 calmodulin, recombinant calmodulin encoded by a synthetic calmodulin gene; F92W/D133E CaM, VU-1 calmodulin mutant in which phenylalanine is replaced by tryptophan at position 92 and aspartate is replaced by glutamate at position 133; 3xCaM, F92W/D95N/S101D/D133E VU-1 calmodulin; 3zCaM, F92W/D95N/N97D/D133E VU-1 calmodulin; 4xCaM, F92W/S101D/D133E VU-1 calmodulin; 4zCaM, F92W/N97D/D133E VU-1 calmodulin; 4xzCaM, F92W/D95N/N97D/S101D/D133E VU-1 calmodulin; cAMP, cyclic adenosine monophosphate; EGTA, ethylene glycol bis( $\beta$ -aminoethyl ether)-*N,N,N',N'*-tetraacetic acid; MOPS, 3-(*N*-morpholino)propanesulfonic acid; PDE, phosphodiesterase; SDS, sodium dodecyl sulfate; Tris, tris(hydroxymethyl)aminomethane.

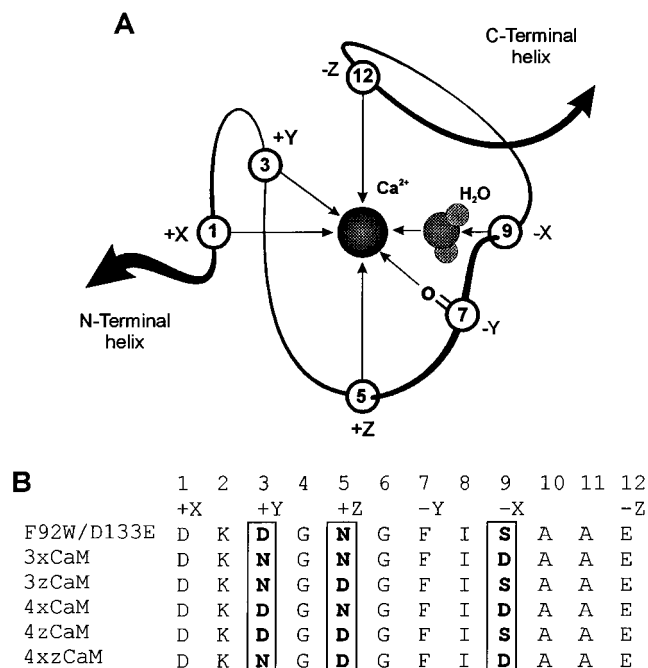


FIGURE 1: (A) Schematic diagram of the loop of a hllh calcium-binding motif. The chelating residues are numbered 1, 3, 5, 7, 9, and 12, and these six positions are denoted as the +X, +Y, +Z, -Y, -X, and -Z positions on the axes of a near-octahedral coordination shell. (B) The amino acid sequences of the calcium binding loop of site III of the CaM mutants. The positions in the loop are numbered 1–12, corresponding to positions 93–104 in CaM. The positions of the chelating residues in the near-octahedral coordination shell are indicated. Mutations are made at the +Y, +Z, and -X positions, and the mutated residues are boldface and boxed.

affinity such as those of CaM sites I–IV, skeletal troponin C sites I and II, and cardiac troponin C site II (6). However, there are exceptions such as the high-affinity EF site of parvalbumin (1). Vogt et al. examined 29 sequences of the hllh motifs from troponin C, myosin light chain, parvalbumin, and CaM (7). They found that the position and linear density of “ $\beta$ -turn-forming” residues in the loop are correlated with the site’s ability to bind calcium. A high propensity of  $\beta$ -turn-forming residues in the first and third tetrapeptides of the loop indicates a possible calcium-binding site. This criterion appears to identify the loops that bind calcium; however, it cannot predict the binding affinity. Boguta et al. proposed a method to estimate calcium binding constants on the basis of the secondary structure of the hllh motif (8). In their procedure, the estimation points are first calculated on the basis of the predicted frequencies of helix, reverse turn, and random coil formation of the residues in a single hllh motif or paired hllh motifs, and then a calcium binding constant is assigned to the site or the paired sites on the basis of the calculated estimation points. This method allows a prediction of calcium binding constants of a typical hllh motif and paired motifs with a precision of 1 order of magnitude. Another quantitative structure/affinity relationship (QSAR) method was established after analyzing six different two-site domains: the N and C domains of rabbit skeletal troponin C, the N and C domains of rabbit CaM, carp parvalbumin, and the C domain of bovine cardiac troponin C (9). This method relates calcium binding affinities ( $1/K_d$ ) of the hllh proteins with the net ligand charge of the two calcium-binding loops, the hydrophobicity of the  $\beta$ -sheet segment of the loops, and the hydrophobicity of the four helices.

Reid and Hodges have proposed the acid pair hypothesis (APH) to correlate the nature of the chelating residues in the loop with the calcium affinity of the hllh calcium-binding motif (10). The APH predicts the calcium affinity of the hllh calcium-binding motif on the basis of the number and location of acidic amino acid residues in chelating positions. This hypothesis states that an hllh calcium-binding site will have a higher affinity for calcium if the anionic ligands in the loop are paired on the axial vertices of a near octahedron than if they are unpaired. Implicit in this hypothesis is the suggestion that a high-affinity calcium-binding site will have a maximum of four acidic residues in positions 1, 3, 5, 9, or 12 in the loop, and these four acidic residues will be paired on the axial vertices of a near octahedron (i.e., the X and Z axes; note that there cannot be a side chain pair on the Y axis since the peptide carbonyl oxygen chelates on the -Y position by definition). This hypothesis has been supported by studies using synthetic 13-residue peptides derived from skeletal troponin C site III (11) and studies using synthetic 33-residue hllh peptide models derived from CaM site III (12, 13). However, the APH does not take into consideration the cooperativity between paired sites, nor does it consider the nonchelating residues in the site or possible interactions with residues outside the site. Therefore, the relevance of the single-site model and hence the APH to calcium binding to hllh motifs in the natural protein remains unknown.

The overall objective of this study was to examine the applicability of the APH to a hllh calcium-binding motif in a whole protein model. Particularly, this study was to examine the effect of structural changes in site III on the calcium affinity of this site using CaM mutants. Since structure/calcium affinity relationships in a multisite protein such as CaM are complicated by cooperativity between the paired sites (2, 4, 5), we cannot directly measure the calcium affinity of site III without the cooperative interference of site IV in CaM. Therefore, it would be helpful to eliminate the cooperative effects on calcium affinity by eliminating calcium binding to site IV. A recent study from our laboratory demonstrates that site IV of CaM is almost inactivated with respect to calcium binding by a D133E mutation at the +Z position of this site (14). In the present study, five CaM mutants (3xCaM, 3zCaM, 4xCaM, 4zCaM, and 4xzCaM) bearing the D133E mutation, in which changes were made to the chelating positions of site III, were designed and prepared to examine the effect of the number and locations of acidic amino acid residues in the chelating positions of site III on the calcium binding affinity of this site with minimum cooperative interference of site IV (Figure 1B). The F92W mutation was maintained in the CaM mutants in order to have a fluorescent label to monitor the calcium-induced structural transitions in the C-terminal domain of the proteins as described previously (14).

Calcium titrations of the CaM mutants were carried out by monitoring the tryptophan fluorescence intensity change. Calcium dissociation constants of sites III and IV in the C-terminal domain of the CaM mutants were calculated from two-site Hill equations fitted to the titration data. Calcium titrations of the CaM mutants were also carried out in the presence of a 26-residue CaM-binding peptide, W4I-M13, to examine the effect of the peptide on the calcium affinity of the CaM mutants. In addition, the effect of the mutations in CaM on its phosphodiesterase (PDE) regulatory activity

was also examined at low (50  $\mu\text{M}$ ) and high (15 mM) calcium concentrations.

## EXPERIMENTAL PROCEDURES

**Construction of the Expression Vectors for Calmodulin Mutants.** The expression vectors for 3xCaM, 3zCaM, 4xCaM, 4zCaM, and 4xzCaM were constructed from plasmid pd133e, an expression vector for F92W/D133E CaM, using site-specific, cassette-mediated mutagenesis as described previously (14, 15). The plasmid vector, pd133e, was constructed previously (14) from the plasmid pVUCH-1, an expression vector for VU-1 CaM (16, 17). Oligonucleotides were synthesized on a Perkin-Elmer Applied Biosystems 391 DNA synthesizer. Positive clones for the CaM mutants were identified by restriction enzyme digestions and automated DNA sequencing on a Perkin-Elmer Applied Biosystems ABI 373A DNA sequencer.

**Preparation of CaM Mutants.** The recombinant CaM mutants were expressed in *Escherichia coli* strain K12 UT481. Each protein was purified from a 20 L culture of the respective positive clone as described previously (14). The homogeneity of the purified proteins was evaluated by SDS-polyacrylamide gel electrophoresis. The identities of the purified proteins were confirmed by amino acid composition analysis using a precolumn phenyl isothiocyanate derivatization HPLC method and molecular weight determination on a VG Quattro Quadrupole mass spectrometer. Protein concentrations were determined by UV spectrophotometry using the extinction coefficient of F92W VU-1 CaM [ $\epsilon_{280\text{ nm}} = 8223\text{ cm}^{-1}\text{ M}^{-1}$ , which was determined previously (14)] for all CaM mutants because the five CaM mutants, F92W/D133E CaM, and F92W VU-1 CaM have one Trp, one Tyr, and eight Phe amino acid residues at identical positions in the proteins.

**Far-UV Circular Dichroism Spectroscopy.** Circular dichroism (CD) spectra were recorded on a Jasco 720 spectropolarimeter at ambient temperature. Each purified protein was dissolved in an EGTA buffer (100 mM KCl, 1 mM EGTA, and 50 mM MOPS at pH 7.20) at concentrations of 20–30  $\mu\text{M}$ , and 0.9 mL of the protein solution was used for each measurement. The water used for preparing the buffer was nanopure water (Barnstead Nanopure II) treated with Chelex 100 resin (Bio-Rad). CD spectra were recorded in the range of 200–250 nm before and after the addition of calcium chloride solution to a final concentration of 40 mM. Data were normalized by the molar concentration of the protein samples and the number of the amino acid residues in the proteins.

**Fluorescence Spectroscopy and Calcium Titration.** Fluorescence emission spectra of the CaM mutants were recorded on a Shimadzu RF540 spectrofluorophotometer at ambient temperature at an excitation wavelength of 282 nm. Calcium titrations of the CaM mutants were carried out by monitoring the tryptophan fluorescence intensity change at an excitation wavelength of 282 nm and an emission wavelength of 340 nm. Spectral measurements and calcium titrations were carried out at protein concentrations of 10  $\mu\text{M}$  in a volume of 2 mL in the EGTA buffer used for CD spectral measurements. For each protein, the spectral measurements were performed before and after the addition of calcium chloride to saturation. The slit width for excitation was 5 nm, and that for emission was 2 nm.

The fluorescence emission spectral measurements and calcium titrations of the CaM mutants were also carried out in the presence of the CaM-binding peptide, W4I-M13. W4I-M13 is a 26-residue peptide analog of the CaM-binding site of the skeletal muscle myosin light chain kinase. The synthesis and purification of W4I-M13 were described elsewhere (14). Protein concentrations were 10  $\mu\text{M}$ , and the protein to peptide ratios were 1:4.

**Calcium Titration Data Analysis.** Free  $\text{Ca}^{2+}$  concentrations were calculated from total  $\text{Ca}^{2+}$  concentrations in the EGTA buffer using the EQCAL program from Biosoft. The logarithmic binding constants ( $\log K$ ) for proton and calcium ion binding to EGTA, used to calculate free calcium concentrations, were as follows:  $\text{H}^+$  to  $\text{EGTA}^{4-}$ , 9.53;  $\text{H}^+$  to  $\text{HEGTA}^{3-}$ , 8.88;  $\text{H}^+$  to  $\text{H}_2\text{EGTA}^{2-}$ , 2.65;  $\text{H}^+$  to  $\text{H}_3\text{EGTA}^-$ , 2.0;  $\text{Ca}^{2+}$  to  $\text{EGTA}^{4-}$ , 10.89; and  $\text{Ca}^{2+}$  to  $\text{HEGTA}^{3-}$ , 5.30. Each set of the fluorescence titration data was fitted to the following one-site (eq 1) and two-site (eq 2) Hill equations using SigmaPlot for Windows:

$$f = \frac{[\text{Ca}^{2+}]^n}{K^n + [\text{Ca}^{2+}]^n} \quad (1)$$

where  $f$  is the fraction of the fluorescence intensity change expressed as the fluorescence intensity change at a given free  $\text{Ca}^{2+}$  concentration from that of apo-CaM over the maximal change during the titration.  $K$  is the average of the apparent calcium dissociation constants of the two sites in the C-terminal domain of CaM, and  $n$  is the slope factor of the titration curve.

$$f = f_1 \frac{[\text{Ca}^{2+}]^{n_1}}{K_1^{n_1} + [\text{Ca}^{2+}]^{n_1}} + (1 - f_1) \frac{[\text{Ca}^{2+}]^{n_2}}{K_2^{n_2} + [\text{Ca}^{2+}]^{n_2}} \quad (2)$$

where  $f_1$  is the fraction of the fluorescence intensity change attributed to one site in the C-terminal domain.  $K_1$  and  $K_2$  are the apparent dissociation constants or the macroscopic dissociation constants of the two sites in the C-terminal domain, respectively, and  $n_1$  and  $n_2$  are the slope factors of the two phases of the titration curve, respectively.

The Hill coefficient ( $n_H$ ) was obtained from the following equation:

$$\log \frac{f}{1-f} = a + n_H \log[\text{Ca}^{2+}]$$

where  $a$  is a constant. This equation was obtained from the central linear part of the Hill plot, namely,  $\log[\text{Ca}^{2+}]$  versus  $\log[f/(1-f)]$ .

**Phosphodiesterase Stimulation Assay.** The five CaM mutants were tested for their regulatory activity in stimulating the CaM-dependent phosphodiesterase (PDE) activity at low (50  $\mu\text{M}$ ) and high (15 mM) calcium concentrations. The PDE stimulation assay was carried out in which the initial hydrolysis rate of cyclic adenosine monophosphate (cAMP) was determined as a function of CaM concentration in an assay buffer containing 0.2 unit/mL of bovine heart PDE, 2 mM [ $^3\text{H}$ ]cAMP, 50  $\mu\text{M}$  or 15 mM  $\text{CaCl}_2$ , 3 mM  $\text{MgSO}_4$ , 100 mM KCl, and 40 mM Tris-HCl at pH 7.5 in a volume of 100  $\mu\text{L}$  as described previously (18). The assay was carried out at 30  $^\circ\text{C}$  for 10 min and terminated in a boiling water bath for 1 min. Snake venom, as a source of nucleotidase, was added to further hydrolyze adenosine

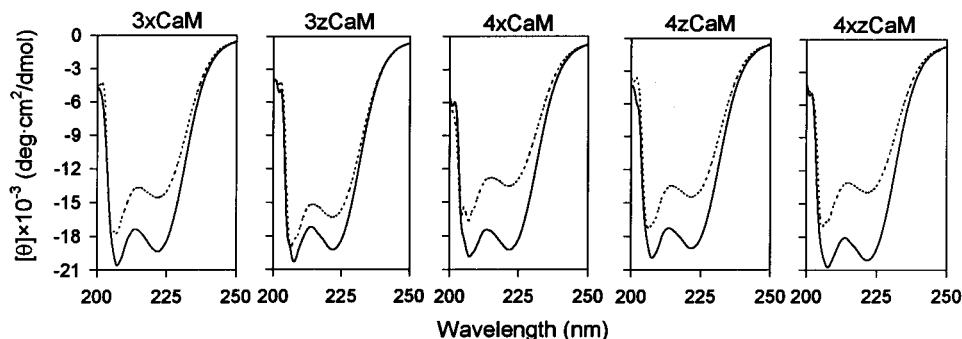


FIGURE 2: Far-UV circular dichroism spectra of CaM mutants. Spectra were recorded at protein concentrations of 20–30  $\mu\text{M}$  in the EGTA buffer (100 mM KCl, 1 mM EGTA, and 50 mM MOPS at pH 7.20) and normalized by molar concentrations of the proteins and the number of amino acid residues in the proteins. The solid lines represent the spectra in the presence of calcium (40 mM), and the dashed lines represent the spectra in the absence of calcium.

Table 1: Molar Ellipticity of CaM Mutants<sup>a</sup>

protein	$-\theta_{222} \times 10^{-3}$ (deg cm <sup>2</sup> dmol <sup>-1</sup> )		$\Delta[\theta]_{222}$
	without Ca <sup>2+</sup>	with Ca <sup>2+</sup>	
F92W CaM <sup>b</sup>	13.76 ± 0.18	17.54 ± 0.03	3.78
F92W/D133E CaM <sup>b</sup>	12.20 ± 0.02	14.09 ± 0.04	1.89
3xCaM	14.58 ± 0.30	19.35 ± 0.26	4.77
3zCaM	16.32 ± 0.16	19.22 ± 0.10	2.90
4xCaM	13.51 ± 0.07	19.22 ± 0.05	5.71
4zCaM	14.45 ± 0.11	19.05 ± 0.04	4.60
4xzCaM	14.01 ± 0.02	20.10 ± 0.03	6.09

<sup>a</sup> Molar ellipticities were determined at 222 nm in the absence and presence of 40 mM calcium chloride. Each value is presented as the mean ± SE (standard error) of three separate measurements. <sup>b</sup> Data from ref 14.

monophosphate to adenosine and phosphate. Bio-Rad AG1-X2 anion exchange resin slurry was added to the reaction mixture to adsorb the unhydrolyzed cAMP. All assays were performed in triplicate, and the PDE stimulation activity was expressed as picomoles of cAMP hydrolyzed per unit of PDE per minute. Data were fitted to the following Hill equation using SigmaPlot for Windows:

$$v = \frac{V_{\max}[\text{CaM}]}{K_{50} + [\text{CaM}]}$$

where  $v$  is the stimulated PDE activity at a given concentration of CaM,  $V_{\max}$  is the maximal stimulated PDE activity, and  $K_{50}$  is the concentration of CaM that is able to produce one-half of the maximal stimulated PDE activity.

Statistical analysis was carried out with an unpaired Student's  $t$  test. A probability ( $p$ ) of less than 0.05 was considered significant.

## RESULTS

**Far-UV Circular Dichroism Spectra.** The normalized far-UV circular dichroism spectra of 3xCaM, 3zCaM, 4xCaM, 4zCaM, and 4xzCaM in the absence and presence of calcium are presented in Figure 2. The overall shapes of the spectra are similar to one another. The corresponding molar ellipticity values and changes in ellipticity at 222 nm are presented in Table 1. Calcium was observed to induce an increase in the magnitude of the negative ellipticities of the five CaM mutants, indicating that calcium induces a change in the structures of the CaM mutants as it does to bovine brain CaM (19) and rabbit skeletal troponin C (20, 21). The differences in the absolute molar ellipticities at 222 nm and

the changes in ellipticities at 222 nm from the calcium-free state to the calcium-bound state of the CaM mutants may indicate the effect of different mutations in the proteins.

**Fluorescence Spectra.** The fluorescence emission spectra of the five CaM mutants recorded in the absence and presence of calcium at an excitation wavelength of 282 nm are shown in Figure 3. A blue shift in the maximal emission wavelength was observed from 342 nm in the absence of calcium to 338 nm in the presence of calcium for the five CaM mutants. Calcium was observed to induce a 1.5–2-fold increase in the tryptophan fluorescence intensity at 340 nm where the largest difference between the emission fluorescence intensity of the apoprotein and that of the Ca<sup>2+</sup>-saturated protein occurred.

The fluorescence emission spectra of the CaM mutants in the presence of W4I-M13 CaM-binding peptide were similar to those obtained in the absence of W4I-M13 peptide (data not shown). However, a blue shift in the maximal emission wavelength was observed from 342 nm in the absence of calcium to 328 nm in the presence of calcium, which was more significant than the calcium-induced blue shift obtained in the absence of W4I-M13 peptide. The calcium-induced increase in the maximal fluorescence intensity in the presence of the peptide was also greater than that obtained in the absence of the peptide (data not shown). These results suggest that the calcium-induced local environment change (to more hydrophobic) of Trp 92 is greater in the presence of the peptide than in the absence of the peptide.

**Calcium Titration.** Each set of calcium titration data was fitted to one-site (eq 1) and two-site (eq 2) models. The two-site model is more appropriate for the data as judged by the fitting coefficients (data not shown), the residuals between the calculated value based on the model and the experimental value of each data point (data not shown), and visual observation. Accordingly, the macroscopic calcium dissociation constants were calculated from each fitted two-site equation (Tables 2 and 3).

In the absence of W4I-M13 peptide, it was observed that biphasic patterns were more pronounced in the titration curves in an ascending order from 3xCaM, 3zCaM, 4xCaM, 4zCaM, and 4xzCaM, indicating that the difference in calcium affinities between sites III and IV in these proteins increases in the same order (Figure 4). Since D → E mutation at the +Z position of synthetic single-site peptides caused either a drastic decrease or a complete loss in the calcium binding capacity in the peptides (22), and the same mutation in site IV of F92W/D133E CaM also decreased

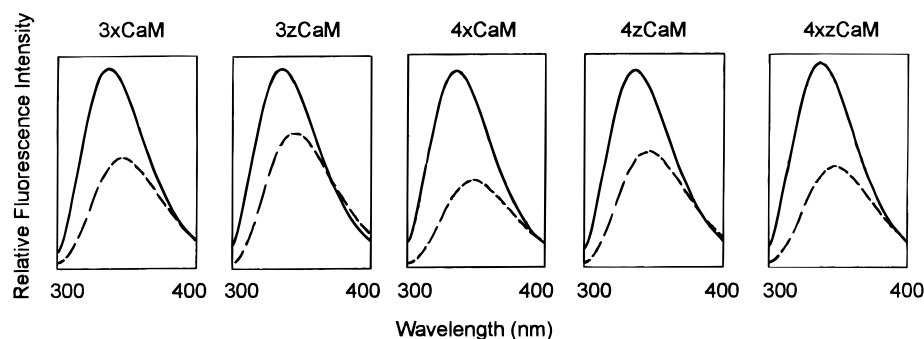


FIGURE 3: Fluorescence emission spectra of CaM mutants. The spectra were recorded at an excitation wavelength of 282 nm. The protein concentrations were 10  $\mu\text{M}$  in the EGTA buffer (100 mM KCl, 1 mM EGTA, and 50 mM MOPS at pH 7.20), and the spectra were recorded before (dashed lines) and after (solid lines) the addition of  $\text{CaCl}_2$  to saturation. The slit width for excitation was 5 nm, and that for emission was 2 nm.

Table 2: Calcium Dissociation Constants of CaM Mutants and Synthetic hIh Calcium Binding Peptides<sup>a</sup>

protein	$K_{\text{III}} (\mu\text{M})$	$K_{\text{IV}} (\mu\text{M})$	$n_{\text{H}}$	peptide <sup>b</sup>	$K_{\text{d}} (\mu\text{M})$
F92W CaM <sup>c</sup>	14 $\pm$ 2.4	1.0 $\pm$ 0.1	1.89		
F92W/D133E <sup>c</sup> CaM	335 $\pm$ 21	2759 $\pm$ 45	0.92	3(DNS)	735 $\pm$ 61 <sup>d</sup>
3xCaM	237 $\pm$ 7	3230 $\pm$ 250	0.70	3x(NND)	524 $\pm$ 16 <sup>d</sup>
3zCaM	140 $\pm$ 11	4461 $\pm$ 69	0.49	3z(NDS)	58.8 $\pm$ 0.1 <sup>d</sup>
4xCaM	5.79 $\pm$ 0.92	859 $\pm$ 64	0.46	4x(DND)	42.1 $\pm$ 1.2 <sup>e</sup>
4zCaM	3.01 $\pm$ 0.09	1846 $\pm$ 24	0.22	4z(DDS)	29.2 $\pm$ 1.0 <sup>e</sup>
4xzCaM	2.09 $\pm$ 0.14	1320 $\pm$ 96	0.13	4xz(NDD)	19.1 $\pm$ 0.2 <sup>d</sup>

<sup>a</sup> Data are presented as the mean  $\pm$  SE of six separate titrations. Subscripts III and IV refer to sites III and IV, respectively, and  $n_{\text{H}}$  is the Hill coefficient. <sup>b</sup> Synthetic hIh calcium binding peptides derived from CaM site III encompassing residues 81–113. The number of acidic amino acid residues, the paired residues on either the X or Z axis or both axes, and the residues in the +Y, +Z, and -X positions in the loop region are indicated in the peptide nomenclature. 3z(NDS), for example, indicates three acidic residues, two of them paired on the z axis, and positions +Y, +Z, and -X occupied by N, D, and S, respectively. <sup>c</sup> Data from ref 14. <sup>d</sup> Data from ref 12. <sup>e</sup> Data from ref 13.

Table 3: Calcium Dissociation Constants of CaM Mutants in the Presence of W4I-M13 CaM Binding Peptide<sup>a</sup>

CaM mutant	$K_1 (\mu\text{M})$	$K_2 (\mu\text{M})$	$n_{\text{H}}$
F92W/D133E CaM <sup>b</sup>	0.358 $\pm$ 0.005	8.13 $\pm$ 0.75	1.99
3xCaM	0.407 $\pm$ 0.001	2.75 $\pm$ 0.24	2.06
3zCaM	0.310 $\pm$ 0.003	5.96 $\pm$ 0.79	1.54
4xCaM	0.202 $\pm$ 0.003	0.977 $\pm$ 0.136	2.20
4zCaM	0.155 $\pm$ 0.001	0.699 $\pm$ 0.071	2.36
4xzCaM	0.122 $\pm$ 0.002	0.625 $\pm$ 0.030	2.03

<sup>a</sup> Each value represents the mean  $\pm$  SE of three separate measurements.  $K_1$  and  $K_2$  are the apparent calcium dissociation constants of CaM obtained in the presence of the CaM-binding peptide, W4I-M13, and  $n_{\text{H}}$  is the Hill coefficient. <sup>b</sup> Data from ref 14.

the calcium affinity of site IV by 2760-fold (14), we assume that the D133E mutation would also cause a drastic decrease in the calcium affinity in site IV of the five CaM mutants. Therefore, the lower calcium dissociation constant was assigned to the higher-affinity site III ( $K_{\text{III}}$ ) and the larger value to the lower-affinity site IV ( $K_{\text{IV}}$ ) (Table 2). The  $K_{\text{III}}$  of these proteins changed significantly in a descending order from 3xCaM, 3zCaM, 4xCaM, 4zCaM, to 4xzCaM, indicating an increase in the calcium affinity in site III in the same order. These results demonstrate that the calcium affinity in site III increases with the increase in the number of acidic chelating residues from three to four, with the increase in the number of acid pairs on the coordinating axes from zero to one and further to two, and with the change of location of the acid pair from the X to the Z axis. The  $K_{\text{IV}}$  values of the CaM mutants were also different from one another, indicating that mutations in site III affect not only the calcium affinity of this site but also that of the partner site (Table 2).

F92W CaM has an  $n_{\text{H}}$  value of greater than 1; however, the other CaM mutants bearing the D133E mutation have

an  $n_{\text{H}}$  value of less than 1 (Table 2). These data indicate that positive cooperativity is present between sites III and IV in F92W CaM but this cooperativity is negative in F92W/D133E CaM, 3xCaM, 3zCaM, 4xCaM, 4zCaM, or 4xzCaM and the negativity increases as the calcium affinity of site III increases. These data further indicate that the positive cooperativity between sites III and IV in CaM has been reversed by the very conservative D133E mutation.

The calcium titration curves obtained in the presence of W4I-M13 peptide are steeper than those obtained in the absence of the peptide (data not shown). The two macroscopic calcium dissociation constants calculated from each fitted curve of the CaM mutants in the presence of W4I-M13,  $K_1$  and  $K_2$ , respectively, are presented in Table 3. Compared to  $K_{\text{III}}$  and  $K_{\text{IV}}$  (Table 2),  $K_1$  and  $K_2$  of the same protein are significantly lower, indicating that the calcium affinity of the CaM mutants is significantly higher in the presence of the CaM-binding peptide than in the absence of the peptide. More interestingly, Hill coefficients of the CaM mutants are all greater than 1 in the presence of W4I-M13 peptide compared to  $n_{\text{H}}$  values that are less than 1 in the absence of the peptide (Tables 2 and 3).

**Phosphodiesterase Stimulation Assay.** At low calcium concentrations (50  $\mu\text{M}$ ), each CaM mutant exhibited a different PDE stimulation curve (data not shown) with different  $V_{\text{max}}$  and  $K_{50}$  values (Table 4). The  $V_{\text{max}}$  changed significantly in an ascending order from 3xCaM, 3zCaM, 4xCaM, to 4zCaM, whereas the  $V_{\text{max}}$  of 4xzCaM was not significantly different from that of 4zCaM. The  $K_{50}$  values of the five CaM mutants ranged from 117 to 234 nM with no consistent pattern. The  $V_{\text{max}}$  values obtained with the five CaM mutants were significantly lower than that obtained with F92W CaM, and the  $K_{50}$  values of the five CaM mutants

Table 4: Phosphodiesterase Stimulation Activity of CaM Mutants<sup>a</sup>

CaM mutant	50 $\mu\text{M}$ $\text{Ca}^{2+}$		15 mM $\text{Ca}^{2+}$	
	$V_{\text{max}}$ (pmol unit <sup>-1</sup> min <sup>-1</sup> )	$K_{50}$ (nM)	$V_{\text{max}}$ (pmol unit <sup>-1</sup> min <sup>-1</sup> )	$K_{50}$ (nM)
F92W CaM <sup>b</sup>	169 $\pm$ 4.8	7.4 $\pm$ 0.7	166 $\pm$ 8	43 $\pm$ 6
F92W/D133E CaM <sup>b</sup>	63.2 $\pm$ 2.5	185 $\pm$ 21	186 $\pm$ 9	41 $\pm$ 4
3xCaM	62.2 $\pm$ 1.4	186 $\pm$ 36	172 $\pm$ 10	34 $\pm$ 2
3zCaM	85.3 $\pm$ 5.4	117 $\pm$ 16	171 $\pm$ 9	34 $\pm$ 2
4xCaM	118 $\pm$ 1	124 $\pm$ 11	190 $\pm$ 6	47 $\pm$ 12
4zCaM	141 $\pm$ 3	234 $\pm$ 39	175 $\pm$ 10	38 $\pm$ 2
4xzCaM	142 $\pm$ 6	134 $\pm$ 23	182 $\pm$ 12	44 $\pm$ 12

<sup>a</sup> Values are presented as the mean  $\pm$  SE of three separate measurements.  $V_{\text{max}}$  is the maximal PDE activity stimulated by CaM, and  $K_{50}$  is the CaM concentration required for a half-maximal stimulated PDE activity. <sup>b</sup> Data from ref 14.

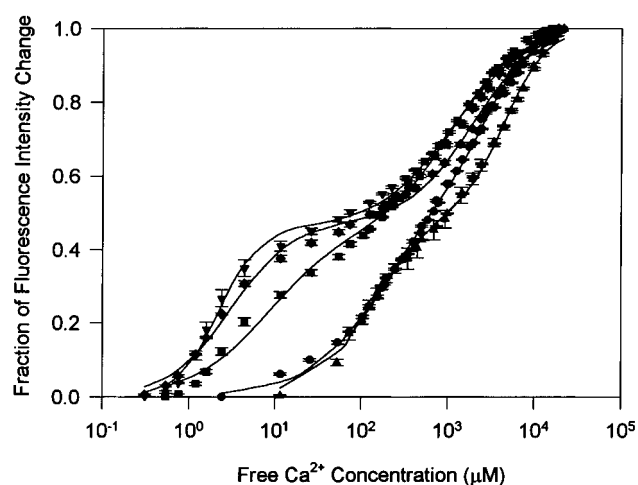


FIGURE 4: Calcium titration curves of CaM mutants. The protein concentration was 10  $\mu\text{M}$  in EGTA buffer (100 mM KCl, 1 mM EGTA, and 50 mM MOPS at pH 7.20) for each CaM mutant. The fluorescence intensity changes were monitored at an excitation wavelength of 282 nm and an emission wavelength of 340 nm. Each data point represents the average of six separate titrations, and the standard error is shown as the error bar. Data were fitted to the two-site model: (●) 3xCaM, (▲) 3zCaM, (■) 4xCaM, (◆) 4zCaM, and (▼) 4xzCaM.

were significantly greater than that of F92W CaM. These results indicate not only that the five CaM mutants have different PDE stimulation activities with variable affinity for the enzyme among themselves but also that all of them have a lower PDE stimulation activity with a lower affinity for the enzyme than that of F92W CaM in the presence of 50  $\mu\text{M}$  calcium. At higher calcium concentrations (15 mM), the PDE stimulation curves of the five CaM mutants were superimposable (data not shown) with similar  $V_{\text{max}}$  and  $K_{50}$  values, which were also similar to those of F92W CaM (Table 4).

## DISCUSSION

Five CaM mutants have been prepared to test the acid pair hypothesis. The mutants are altered in the +Y, +Z, and -X chelating residue positions of site III to produce products that have either three or four acidic amino acid residues in chelating positions with the acidic residues paired on the X and/or Z axis (Figure 1). Two other distinguishing features of the five mutants are relevant to their calcium binding characteristics. First, all mutants carry the D133E mutation that has been demonstrated to drastically reduce the calcium affinity of site IV (14). Since site IV is cooperatively paired with site III in the C-terminal domain of calmodulin, this mutation was designed to eliminate cooperativity between

these two sites. Second, Phe 92 which immediately precedes the loop region of site III is replaced by a Trp residue to insert a fluorescent label to monitor the calcium-induced conformational transitions in the C-terminal domain (14, 23). An examination of the calcium dissociation constants of site III ( $K_{\text{III}}$ ) in each of the mutants shows that the 4xzCaM mutant has the highest calcium affinity followed by 4zCaM, 4xCaM, 3zCaM, 3xCaM, and F92W/D133E CaM. These results demonstrate that the number and location of the acidic residues in the chelating positions of site III significantly affect the calcium affinity of this site (Table 2).

The  $K_{\text{III}}$  values of the mutants with three acidic residues in chelating positions (see F92W/D133E CaM, 3xCaM, and 3zCaM in Figure 1 and Table 2) are significantly higher when compared to the  $K_{\text{III}}$  values of those mutants with four acidic residues in chelating positions (see 4xCaM, 4zCaM, and 4xzCaM in Figure 1 and Table 2). The data indicate that a hll calcium-binding site with four acidic residues in the chelating positions has a higher affinity for calcium than a site with three acidic chelating residues. This provides experimental support of the APH postulate stating that loops with four acidic chelating residues will have a higher calcium affinity than those with three acidic chelating residues (10).

Mutants with four acidic chelating residues in site III may have two acid pairs with one on each of the X and Z axes (see 4xzCaM in Figure 1 and Table 2), one acid pair on the Z axis (4zCaM), or one acid pair on the X axis (4xCaM). The fact that the  $K_{\text{III}}$  for 4xzCaM is 1.4- and 2.8-fold lower than those of 4zCaM and 4xCaM, respectively, indicates that a hll calcium-binding site with two acid pairs on the X and Z axes has a higher calcium affinity than a site with one acid pair on either the X or Z axis (Table 2). A possible interpretation of this data is that, when four acidic residues are present in the  $\pm X$  and  $\pm Z$  positions (4xzCaM), the dentates are optimally separated and minimal electrostatic repulsion would result. When four acidic residues are present in the  $\pm X$ , +Y, and -Z positions (4xCaM) or in the +X, +Y, and  $\pm Z$  positions (4zCaM), two dentates in the +X and +Y or the +Y and +Z positions could possibly interact through electrostatic repulsion, leading to a less stable inner sphere complex with the cation and a lower calcium affinity (Figure 1).

Among the CaM mutants which have three acidic chelating residues in site III, the  $K_{\text{III}}$  of F92W/D133E CaM is 1.4- and 2.4-fold greater than those of 3xCaM and 3zCaM, respectively. This indicates that a hll calcium-binding site with one acid pair on either the X axis or Z axis has a higher affinity for calcium than a site with no acid pairs (Table 2). This observation can also be explained as the unfavorable situation due to the dentate-dentate repulsion that may occur

when two acidic residues are located at neighboring chelating positions in the sequence as in the case of F92W/D133E CaM (+X and +Y positions occupied by Asp), whereas such electrostatic repulsion would not be predominant in 3xCaM and 3zCaM (Figure 1).

The demonstration that the  $K_{III}$  of 3zCaM is 1.7-fold lower than that of 3xCaM and the  $K_{III}$  of 4zCaM is 1.9-fold lower than that of 4xCaM (Table 2) indicates that a hlh calcium-binding site with one acid pair on the Z axis has a higher affinity for calcium than a site with one acid pair on the X axis. This observation could be due to the fact that the residue in the  $-X$  position is indirectly involved in the chelation of calcium through a water molecule (2–5). As a result, the X acid pair contributes less negative charge in stabilizing the complex, leading to a calcium affinity lower than that of the Z acid pair.

To date, it would appear that the acid pair is limited to Asp-Asp on the X axis and Asp-Glu on the Z axis. A Glu-Glu acid pair on the Z axis has been shown to be detrimental to calcium affinity of the respective site in the CaM mutants in this study and in previous studies (14, 22). These results demonstrate that both the number and location of the acidic chelating residues as well as the type of acidic residue are critical to the calcium affinity. Since the APH does not consider the type of acidic amino acid residue in the chelating positions, the result of reduction in calcium binding to hlh motifs with Glu in the +Z position is not predicted and appears to invalidate the hypothesis. This aspect of the APH is currently under investigation in our laboratory.

The  $K_{III}$  of the CaM mutants from the present study is compared to the calcium dissociation constant,  $K_d$ , of the synthetic single-site calcium-binding peptides derived from CaM site III (Table 2). All the 33-residue single-site peptides 3(DNS), 3x(NND), 3z(NDS), 4x(DND), 4z(DDS), and 4xz(NDD) have amino acid sequences in the loop identical to those in site III of the CaM mutants F92W/D133E CaM, 3xCaM, 3zCaM, 4xCaM, 4zCaM, and 4xzCaM, respectively, with the exception being that the Tyr located in the  $-Y$  position in the peptides is replaced by a Phe in the proteins. By comparing the  $K_d$  of each single-site peptide model with the  $K_{III}$  of the whole protein model [for example, compare 3(DNS) with F92W/D133E CaM], we find that the  $K_{III}$  of the whole protein model changes with the nature of the chelating residues in the site in a fashion similar to that of the changes in the  $K_d$  of the single site peptide model. These results demonstrate that the nature of the chelating residues, particularly the number and location of the acidic residues in the chelating positions, affects the calcium affinity in the whole protein model in a manner similar to that of the isolated single-site peptide model. The peptide model  $K_d$  values are greater than their respective protein model  $K_{III}$  values by a factor of 2.2–9.7 except for the 3z(NDS) and 3zCaM pair, indicating that there are still other interactions in the whole protein model that contribute to the increased calcium affinity of the site in the whole protein. The reason why the 3z(DNS) peptide has a 2.4-fold higher affinity for calcium than the 3zCaM protein is not clear at this moment but may possibly be a symptom of the reversal of cooperativity found in the mutants and discussed below. Although the whole protein model and the isolated single-site model are not identical in terms of the calcium affinity of the respective sites, the data from the present study and from the previous studies using the synthetic single-site peptides

demonstrate that the single hlh motif can be used as a valid model to study structure/calcium affinity relationships of the hlh motifs in calcium-binding proteins (12, 13).

Unlike  $K_{III}$ ,  $K_{IV}$  did not show any consistent pattern in the different mutant proteins (Table 2). However, analysis of the Hill plots of the calcium titration of each mutant indicates that there is positive cooperativity in the F92W mutant that is lost in the F92W/D133E mutant as a result of the D133E mutation. It is noteworthy that the subsequent mutants that have progressively increasing calcium affinities in site III also have a corresponding decrease in the Hill coefficient (Table 2). This is indicative of an increasing negative cooperativity as we increase the calcium affinity of site III. It would appear that the order of site filling in the natural protein (F92W and VU-1 CaM) which is site IV  $\rightarrow$  site III is positively cooperative; however, reversing the order of filling of the sites (site III  $\rightarrow$  site IV) produces negative cooperativity between the sites. Positive cooperativity is restored in all mutants when the sites are titrated in the presence of the CaM-binding fragment of myosin light chain kinase, W4I-M13 (Table 3). The full implication of these results for the biological role of calcium regulation of calmodulin and the erratic behavior of  $K_{IV}$  in these mutants is currently under investigation.

The macroscopic calcium binding affinity of the five CaM mutants is also increased in the presence of the CaM-binding peptide (Table 3). This result is consistent with previous studies in which W4I-M13 peptide increased the calcium affinity of VU-1, F92W, and F92W/D133E calmodulins (14). The CaM-binding peptide, mastoparan, and the CaM-binding fragment of caldesmon have been shown to increase the calcium affinity of scallop testis CaM (24). Another CaM-binding peptide, RS20, has also been shown to increase the calcium affinity of VU-1, E67A, and E140A calmodulins (25). CaM-binding peptides are believed to stabilize the calcium-bound form of CaM and increase the positive cooperativity between the N- and C-terminal domains, thereby increasing the calcium affinity of CaM (14, 24).  $K_1$  and  $K_2$  may not necessarily represent the calcium binding affinity of sites III and IV due to the aforementioned positive cooperativity between the N- and C-terminal domains. Alternatively, they may reflect calcium binding to the N- and C-terminal domains, respectively. As a result, we are not able to determine if the sequence of site filling reverts to the original IV  $\rightarrow$  III sequence or remains as the III  $\rightarrow$  IV sequence. It is also possible that the positive cooperativity indicated by the Hill coefficients is a result of the interaction between the N- and C-terminal domains (Table 3).

The PDE regulatory activities of the five CaM mutants were also examined in the presence of low (50  $\mu$ M) and high (15 mM) calcium concentrations (Table 4). At 50  $\mu$ M calcium, 3xCaM, 3zCaM, 4xCaM, 4zCaM, and 4xzCaM stimulate PDE to different maximal levels with different affinities for the enzyme (Table 4). The higher the calcium affinity of site III of the CaM mutant, the more efficient the protein is in PDE regulation. However, these CaM mutants are still less efficient in PDE regulation than F92W CaM in the presence of 50  $\mu$ M calcium. On the contrary, all five CaM mutants exhibit a similar PDE regulatory activity with a similar affinity for the enzyme to F92W CaM when the calcium concentration increases to 15 mM (Table 4). These results are consistent with those obtained with F92W/D133E CaM and demonstrate not only that the calcium-bound form

of CaM is essential for PDE regulation but also that the multiple mutations alter calcium regulation of the CaM-mediated PDE activity without affecting CaM interaction with the enzyme.

To summarize, this study demonstrates the limited application of the APH in predicting the cation affinities of a multisite calcium binding protein. Conclusions drawn from earlier studies on synthetic models of a single hlh cation-binding site describing the effects of the number and location of acidic residues in chelating positions of the loop on the cation affinity appear to be applicable to the multisite protein. The fact that the D133E mutation drastically reduces the cation affinity of site IV indicates that the type of acidic residue in chelating positions also plays a role in dictating the cation affinity of the hlh site. This mutation has also been useful in providing the opportunity for an interesting look at the possible relationship between the sequence of filling the calcium binding sites and cooperative interactions between the sites. The IV  $\rightarrow$  III sequence exhibits positive cooperativity, while the III  $\rightarrow$  IV sequence exhibits negative cooperativity. Although the calcium-binding loop provides a primary control of the cation binding parameters and the APH provides a basis for qualitatively predicting the importance of particular loop residues for the calcium affinity of the hlh calcium-binding motif, evidence also suggests that other regions of the hlh motif also provide important control elements (4, 5). This study also demonstrates that the multiple mutations in site III alter the calcium affinity without affecting CaM interaction with the enzyme.

#### ACKNOWLEDGMENT

We are grateful to Dr. Daniel Roberts, who originally synthesized the CaM gene, Dr. Thomas Lukas for generously providing the plasmid pVUCH-1 and *E. coli* strain K12 UT481, and Dr. Grant Mauk for the use of his Jasco J720 CD spectropolarimeter. We also thank Mr. Roland Burton for performing the mass spectrometry molecular weight determinations and Mr. Patrick Franchini for many stimulating discussions and great help in preparing the figures of the manuscript.

#### REFERENCES

1. Kretsinger, R. H., and Nockolds, C. E. (1973) *J. Biol. Chem.* 243, 3313–3326.
2. Strynadka, N. C. J., and James, M. N. G. (1989) *Annu. Rev. Biochem.* 58, 951–998.

3. McPhalen, C. A., Strynadka, N. C. J., and James, M. N. G. (1991) *Adv. Protein Chem.* 42, 77–144.
4. Falke, J. J., Drake, S. K., Hazard, A. L., and Peersen, O. B. (1994) *Q. Rev. Biophys.* 27, 219–290.
5. Linse, S., and Forsén, S. (1995) *Adv. Second Messenger Phosphoprotein Res.* 30, 89–151.
6. Potter, J. D., Johnson, J. D., Dedman, J. R., Schreiber, W. E., Mandel, F., Jackson, R. L., and Means, A. R. (1977) in *Calcium Binding Proteins and Calcium Function* (Wasserman et al., Eds.) pp 239–250, Elsevier North-Holland Inc., New York.
7. Vogt, H.-P., Strassburger, W., and Wollmer, A. (1979) *J. Theor. Biol.* 76, 297–310.
8. Boguta, G., Stepkowski, D., and Bierzynski, A. (1988) *J. Theor. Biol.* 135, 41–61.
9. Sekharudu, Y. C., and Sundaralingam, M. (1988) *Protein Eng.* 2, 139–146.
10. Reid, R. E., and Hodges, R. S. (1980) *J. Theor. Biol.* 84, 401–444.
11. Marsden, B. J., Hodges, R. S., and Sykes, B. D. (1988) *Biochemistry* 27, 4198–4206.
12. Reid, R. E. (1990) *J. Biol. Chem.* 265, 5971–5976.
13. Procyshyn, R. M., and Reid, R. E. (1993) *J. Biol. Chem.* 269, 1641–1647.
14. Wu, X., and Reid, R. E. (1997) *Biochemistry* 36, 3608–3616.
15. Craig, T. A., Watterson, D. M., Prendergast, F. G., Haiech, J., and Roberts, D. M. (1987) *J. Biol. Chem.* 262, 3278–3284.
16. Roberts, D. M., Crea, R., Malecha, M., Alvarado-Urbina, G., Chiarello, R. H., and Watterson, D. M. (1985) *Biochemistry* 24, 5090–5098.
17. Lukas, T. J., Craig, T. A., Roberts, D. M., Watterson, D. M., Haiech, J., and Prendergast, F. G. (1987) in *Calcium-Binding Proteins in Health and Disease* (Norman, A. W., et al., Eds.) pp 533–543, Academic Press, New York.
18. Wallace, R. B., Tallant, E. A., and Cheung, W. Y. (1983) *Methods Enzymol.* 102, 39–47.
19. Drabikowski, W., Brzeska, H., and Venyaminov, S. Y. (1982) *J. Biol. Chem.* 257, 11584–11590.
20. Johnson, J. D., and Potter, J. D. (1978) *J. Biol. Chem.* 253, 3775–3777.
21. McCubbin, W. D., Oikawa, K., Sykes, B. D., and Kay, C. M. (1982) *Biochemistry* 21, 5948–5956.
22. Reid, R. E., and Procyshyn, R. M. (1995) *Arch. Biochem. Biophys.* 323, 115–119.
23. Trigo-Gonzalez, G., Racher, K., Burtnick, L., and Borgford, T. (1992) *Biochemistry* 31, 7009–7015.
24. Yazawa, M., Ikura, M., Hikichi, K., Ying, L., and Yagi, K. (1987) *J. Biol. Chem.* 262, 10951–10954.
25. Haiech, J., Kilhoffer, M.-C., Lukas, T. J., Craig, T. A., Roberts, D. M., and Watterson, D. M. (1991) *J. Biol. Chem.* 266, 3427–3431.

BI970278C